

Thermodynamic Characterization of the Interaction of Mutant UvrB Protein with Damaged DNA

Huaxian Ma and Yue Zou*

Department of Biochemistry and Molecular Biology, James H. Quillen College of Medicine, East Tennessee State University, Johnson City, Tennessee 37614

Received November 7, 2003; Revised Manuscript Received February 5, 2004

ABSTRACT: During the DNA damage recognition of nucleotide excision repair in *Escherichia coli* the interaction of UvrB protein with damaged DNA ensures the recognition of differences in the intrinsic chemical structures of a variety of adduct molecules in DNA double helix. Our earlier study indicated that a single tyrosine-to-tryptophan mutation at residue 95 converted the UvrB to a protein [UvrB(Y95W)] that is able to bind to a structure-specific bubble DNA substrate, even in the absence of UvrA. Fluorescence spectroscopy therefore was adopted to investigate the biochemical properties and thermodynamics of DNA damage recognition by the mutant protein. We examined the binding of the UvrB(Y95W) mutant protein to a structure-specific 30 bp DNA substrate containing a single fluorescein which serves as both an adduct and a fluorophore. Binding of the protein to the substrate results in a significant reduction in fluorescence. By monitoring the fluorescence changes, binding isotherms were generated from a series of titration experiments at various physiological temperatures, and dissociation constants were determined. Analysis of our data indicate that interaction of UvrB(Y95W) protein with the adduct incurred a large negative change in heat capacity ΔC_p° ($-1.1 \text{ kcal mol}^{-1} \text{ K}^{-1}$), while the $\Delta G^{\circ}_{\text{obs}}$ was relatively unchanged with temperature. Further study of the binding at various concentrations of KCl showed that on average only about 1.5 ion pairs were involved in formation of the UvrB–DNA complex. Together, these results suggested that hydrophobic interactions are the main driving forces for the recognition of DNA damage by UvrB protein.

One of the most striking features of nucleotide excision repair (NER)¹ is its capability of removing a large variety of bulky DNA adducts with varying efficiencies (1–3). This unique feature as compared to other DNA repair pathways in cells is delivered by the remarkable DNA damage recognition system of NER. This is best illustrated by the well-documented system of *Escherichia coli* NER. In this system, recognition of DNA adducts is achieved through a sequential two-step mechanism in which the adduct-induced disruption of Watson–Crick helical structure is recognized at the initial step, most likely by the UvrA₂ subunit of the UvrA₂B complex, while the type of modifications of the nucleotide is recognized by UvrB at the following step upon strand separation (4). The role of UvrB is central to the process as the protein is directly involved in the interaction with the adduct molecules. As a multifunctional protein in *E. coli* NER, UvrB also interacts with UvrA and UvrC proteins progressively through the course of damage processing and incision by the UvrABC system.

There has been a long interest in understanding the biochemical basis of UvrB interaction with DNA adducts and its roles in damage recognition of *E. coli* NER. As one of the major efforts, crystal structures of UvrB proteins from *Bacillus caldopenax* and *Thermus thermophilus* bacteria have

been solved recently at high resolutions (5–7). These studies revealed some interesting structural features of the UvrB proteins, particularly a β -hairpin loop which is located in a molecular cleft in UvrB. While it has been suggested that this β -hairpin loop and the cleft are involved in DNA binding and damage recognition, the biochemical features of how a DNA adduct is recognized by UvrB remain unclear. It was difficult to study the direct interaction of the UvrB with DNA because of the requirement of UvrA and ATP hydrolysis for the formation of the UvrB–DNA complex. The involvement of UvrA and ATP hydrolysis significantly complicates the determination of UvrB interaction with DNA adducts.

In an attempt to overcome these obstacles, we reported in the accompanying paper that a single amino acid change at residue 95 of UvrB from tyrosine to tryptophan (Y95W) made the protein capable of binding to structure-specific DNA substrates without the involvement of UvrA (26). This binding was comparable to that of the native UvrB in the presence of UvrA. Furthermore, this mutant protein is fully functional in NER as compared with the native protein. Considering the crucial role of UvrB in *E. coli* NER, here we examined the thermodynamics of the damage recognition by UvrB using fluorescence spectroscopy. In comparison to many pseudoequilibrium methods used in studies of protein–DNA interactions, fluorescence spectroscopy is a rigorous noninvasive approach and delivers true equilibrium measurement of the interactions. In the present study fluorescence from either tryptophan of residue 95 (introduced into UvrB

* To whom correspondence should be addressed. Phone: (423) 439-2124. Fax: (423) 439-2030. E-mail: zouy@etsu.edu.

¹ Abbreviations: DTT, dithiothreitol; EDTA, ethylenediaminetetraacetic acid; NER, nucleotide excision repair.

by the mutation) or fluorescein (an adduct and a good substrate of UvrABC nuclease) was monitored. By systematically changing the temperature and ionic strength of the buffer, we have determined the thermodynamic parameters of the UvrB mutant binding to the fluorescein–DNA adduct. The molecular accessibility of specific residues of the UvrB protein in the presence and absence of DNA substrate also was probed using the method of fluorescence quenching by acrylamide.

EXPERIMENTAL PROCEDURES

Proteins and DNA Substrates. The UvrB, UvrB(Y92W), UvrB(Y95W), and UvrB(Y101W) mutant proteins were purified as described previously (26). The fluorescein-labeled 30 bp (F–30 bp) bubble substrate used in this study was constructed and purified as reported earlier (26). The substrate was composed of two strands, 5′-CCATCFCTACCGCAATCAGGCCAGATCTGC and 5′-GCAGATCTGGCCTGATTGCGGCTTTTCTGG, where F stands for fluorescein and the underlined bases indicate the location of mismatches for the bubble formation.

Fluorescence Measurement. The fluorescence measurements were performed on a SPEX Fluorolog-3 fluorometer (Jobin Yvon Inc.) with the slit widths set at 1 and 5 nm for excitation and emission beams, respectively, for fluorescein and at 3 and 5 nm, respectively, for tryptophan. The tryptophan fluorescence was recorded with $\lambda_{\text{ex}} = 295$ nm and $\lambda_{\text{em}} = 350$ nm, and the fluorescein fluorescence was recorded at $\lambda_{\text{ex}} = 492$ nm and $\lambda_{\text{em}} = 520$ nm. No more than 5% photobleaching was observed under these conditions. All titrations were performed in a micro quartz cuvette (4 × 4 mm; 200 μ L) with a 2 × 2 mm stirring bar.

Fluorescence quenching experiments were conducted for UvrB proteins (1 μ M) site-specifically mutated with a single tryptophan. Briefly, the proteins were titrated with varying concentrations of acrylamide quencher at 25 °C in the presence or absence of the F–30 bp bubble substrate in a buffer containing 50 mM Tris-HCl, pH 8.0, 5 mM EDTA, 10 mM MgCl₂, 50 mM KCl, and 10% glycerol. The fluorescence of tryptophan was monitored. The fluorescence data were analyzed by the Stern–Volmer equation

$$F_0/F = 1 + K_{\text{sv}}[Q]$$

where F_0 and F are the unquenched and the quenched fluorescence intensities, respectively. The term $[Q]$ is the molar concentration of the collisional quencher, which is the acrylamide in this case. K_{sv} is the Stern–Volmer dynamic quenching constant.

For the temperature- and ion-dependent measurements, fluorescence titration of the F-30bp bubble substrate (0.1 μ M), upon each addition of UvrB(Y95W), was carried out by measuring $\lambda_{\text{ex}} = 520$ nm with $\lambda_{\text{em}} = 492$ nm. The binding reaction was conducted in a microcuvette containing 200 μ L of buffer [50 mM Tris-HCl, pH 8.0, 50 mM KCl (or as indicated), 5 mM EDTA, 10 mM MgCl₂, and 10% glycerol] at given temperatures. In these experiments, UvrB(Y95W) and the DNA substrate were placed in the same binding buffer before the titration so that the background did not change during the addition of protein. Each addition of protein was delivered as a 1 μ L aliquot from a 25 μ L Hamilton syringe using a Hamilton repeating dispenser. The

cuvette temperature was controlled by a LFI-3751 Peltier temperature controller (Wavelength Electronics, Inc.).

Determination of Thermodynamic Parameters. Data collected from the fluorescence titration experiments were analyzed to determine the equilibrium dissociation constants ($K_{\text{d,obs}}$) or binding constant (K_{obs}) and other thermodynamic parameters.

For processes with a large magnitude of temperature-independent ΔC_p° , the thermodynamics can be completely characterized by ΔC_p° and two characteristic temperatures, T_H (where $\Delta H^{\circ}_{\text{obs}} = 0$), and T_S (where $\Delta S^{\circ}_{\text{obs}} = 0$) (8–11):

$$\ln K_{\text{obs}} = \frac{\Delta C_p^{\circ}}{R} \left[\frac{T_H}{T} - \ln \frac{T_S}{T} - 1 \right] \quad (1)$$

To obtain the value of ΔC_p° , the van't Hoff plot of experimental data was best fitted with the above equation using a nonlinear least-squares method.

The temperature dependence of K_{obs} also was used to calculate the Gibbs free energy change:

$$\Delta G^{\circ} = -RT \ln K_{\text{obs}} \quad (2)$$

Also at the equilibrium

$$-R \left[\frac{\partial \ln K_{\text{obs}}}{\partial (1/T)} \right]_p = \Delta H^{\circ}_{\text{obs}} \quad (3)$$

and

$$\frac{\partial \Delta G^{\circ}_{\text{obs}}}{\partial T} = -\Delta S^{\circ}_{\text{obs}} \quad (4)$$

Thus the standard enthalpy and entropy changes can be defined by

$$\Delta H^{\circ}_{\text{obs}} = \Delta C_p^{\circ} (T - T_H) \quad (5)$$

$$\Delta S^{\circ}_{\text{obs}} = \Delta C_p^{\circ} \ln(T/T_S) \quad (6)$$

These thermodynamic relationships permit a full analysis of thermodynamic parameters for the system examined.

Ion Effect Analysis. The salt dependence of the specific binding of UvrB(Y95W) to the F–30 bp DNA substrate was determined by conducting titration experiments in buffer solutions with different KCl concentrations. The analysis of these data to determine the equilibrium binding constants was the same as that described above. The effect of the salt concentration on complex formation has been described by the relationship:

$$\frac{\partial \ln K_{\text{obs}}}{\partial \ln [M^+]} = -m'\psi \quad (7)$$

where m' is the number of ion pairs formed and ψ is the fraction of counterions bound per phosphate which is assumed to be 0.88 for double helical DNA (12–14). $[M^+]$ is the concentration of the monovalent metal ion of salt.

RESULTS

Fluorescence Quenching of UvrB Mutant Proteins by Acrylamide. As reported earlier (26), a single replacement of tyrosine with tryptophan at residue 95 rendered the UvrB

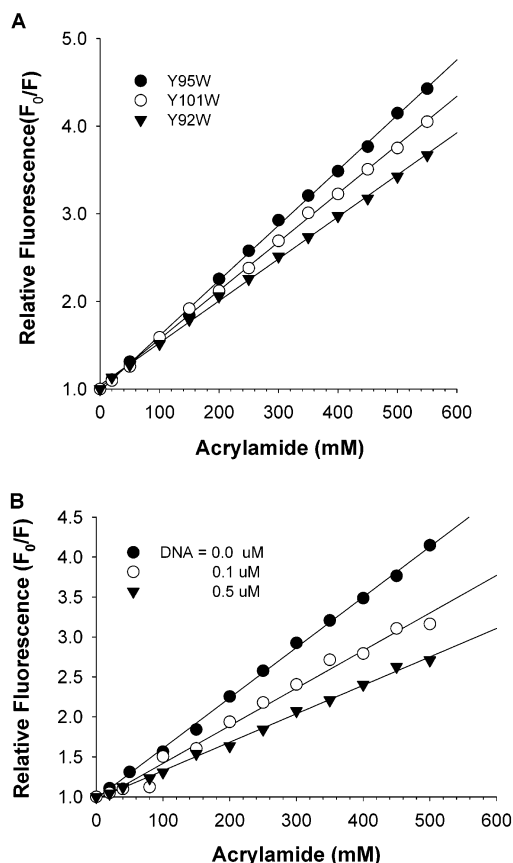


FIGURE 1: Stern–Volmer plots of tryptophan fluorescence quenching of UvrB mutant proteins by acrylamide. Experiments were conducted as described under Experimental Procedures. Panel A: Fluorescence quenching of UvrB(Y92W), UvrB(Y95W), and UvrB(Y101W) by acrylamide. The Stern–Volmer constants (K_{sv}) are 6.3 ± 0.5 , 5.5 ± 0.3 , and 4.8 ± 0.2 M^{-1} for Y95W, Y101W, and Y92W proteins, respectively. Panel B: Fluorescence quenching of UvrB(Y95W) by acrylamide in the presence and absence of DNA substrate. The Stern–Volmer constants are 6.3, 4.7, and 3.6 M^{-1} in the absence and presence of 0.1 and 0.5 μ M DNA substrate, respectively.

protein capable to bind to the DNA substrate directly, while similar mutations at other sites (Y92, Y96, and Y101) in the same β -hairpin exhibited no such effect. Since the β -hairpin appears to be directly involved in damage recognition and DNA interaction, these residues therefore may play different roles in the interaction. To better understand the biochemical properties of these residues in the functions of UvrB protein, fluorescence quenching experiments were performed. Fluorescence quenching has been used widely to determine the aqueous accessibility of protein residues, as well as the chemical features of these residues (15). As shown in Figure 1, the tryptophan fluorescence of the mutants Y92W, Y95W, and Y101W of UvrB was quenched with varying concentrations of acrylamide (native UvrB contains no tryptophan). Acrylamide is a polar uncharged (neutral) fluorescence quencher (15–17). The extent of fluorescence quenching (F_0/F) (at $\lambda_{em} = 350$ nm) of the mutant proteins was plotted as a function of acrylamide concentrations (Figure 1A). Regardless of the experimental conditions, plotting F_0/F as a function of acrylamide concentration results in a straight line extrapolating to a value near 1 at zero concentration of the quencher. As shown in Figure 1A, the efficiency of fluorescence quenching follows the order of Y95W > Y101W > Y92W. Further analysis of the data with

Table 1: Temperature Dependence of the Interaction of UvrB(Y95W) with DNA Adduct

T ($^{\circ}C$)	K_{obs} (M^{-1})
16	$2.69 (\pm 0.14) \times 10^6$
20	$4.48 (\pm 0.66) \times 10^6$
25	$10.85 (\pm 2.43) \times 10^6$
30	$11.04 (\pm 1.22) \times 10^6$
37	$11.31 (\pm 0.47) \times 10^6$

the Stern–Volmer equation, $F_0/F = 1 + K_{sv}[Q]$ (15), indicated that the Stern–Volmer constants for collisional quenching K_{sv} are 6.3 ± 0.5 , 5.5 ± 0.3 , and 4.8 ± 0.2 M^{-1} , for Y95W, Y101W, and Y92W UvrB proteins, respectively. These results indicated that residue 95 is not only fairly accessible to the aqueous solution but also more accessible than residues 92 and 101, which is consistent with its unique role in the interaction with DNA substrate (26).

The fluorescence quenching of the UvrB(Y95W) protein by acrylamide also was examined in the presence of DNA substrate. As shown in Figure 1B, the presence of DNA or the binding of the UvrB(Y95W) protein to DNA reduced the fluorescence quenching efficiency and thus the solvent accessibility of residue 95 in comparison with the case in the absence of DNA. The partial loss of accessibility was most likely due to the direct contact of residue 95 with DNA which shielded the residue to some extent from collision with aqueous molecules.

Binding of UvrB(Y95W) Protein to the DNA Adduct at Varying Temperatures. The measurement of the equilibrium constant K_{obs} as a function of temperature provides a convenient approach to determine the thermodynamic properties of protein–DNA interactions, including ΔG°_{obs} , ΔH°_{obs} , ΔS°_{obs} , and $\Delta C_p^{\circ}_{obs}$. Changes of these thermodynamic state functions are the results of all molecular interactions involved in the binding and provide information about the intrinsic properties of the process (10). As shown in Table 1, the equilibrium constants for the interaction of UvrB(Y95W) with the fluorescein–30 bp (F–30 bp) bubble substrate (26) were determined over a temperature range of 16–37 $^{\circ}C$. In these experiments, the quenching of the fluorescein fluorescence ($\lambda_{ex} = 492$ nm, $\lambda_{em} = 520$ nm) upon binding of the protein was monitored and recorded. The fluorescein in the substrate served for two purposes, one as an adduct which is a good substrate of NER and is incised efficiently by UvrABC nuclease (data not shown) and the other as a fluorophore to track molecular interactions. At given temperatures, binding isotherms were generated from titration of the DNA substrate with the UvrB(Y95W) protein and were best fitted with the one-binding model for calculation of equilibrium constants using a nonlinear least-squares method (18) (at least three independent determinations). This set of temperature-dependent data was then subjected to a van't Hoff plot in which the natural log of the equilibrium constants for the UvrB(Y95W)–DNA interaction was plotted as a function of the reciprocal of temperatures, K (Figure 2). The specific binding of UvrB(Y95W) to the F–30 bp substrate is characterized by a nonlinear van't Hoff plot, different from many chemical reactions which have a linear van't Hoff plot and constant enthalpy over such a narrow temperature range. This nonlinear relationship is most likely due to the temperature dependency of the standard enthalpy change upon binding (eq 3). As shown in Figure

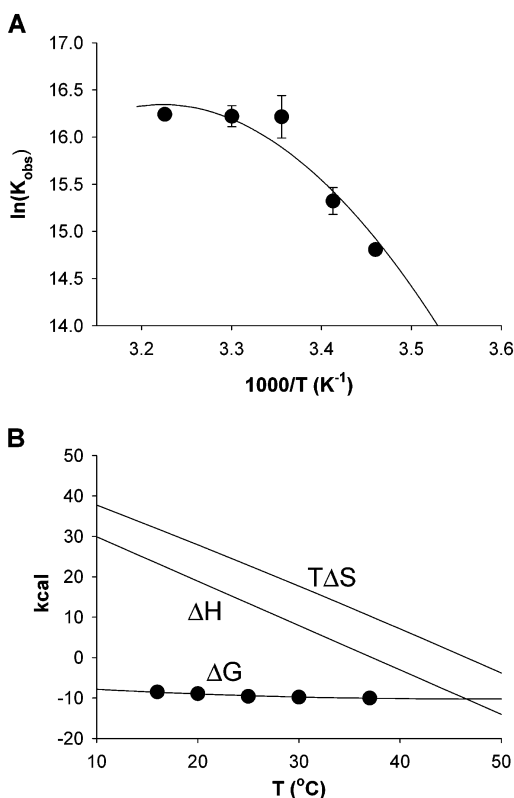


FIGURE 2: Panel A: van't Hoff plot of UvrB(Y95W) binding to the F–30 bp bubble substrate. The experiments were conducted as described in Experimental Procedures. The error bars indicate the standard deviation of at least three independent determinations. Some of the error bars are too small to see as compared with the symbols of experimental data. Panel B: Entropy, enthalpy, and free energy changes of the specific interaction of UvrB(Y95W) with DNA substrate as a function of temperature. Values of ΔH , ΔS , and ΔG_{obs} were obtained from eqs 2, 5, and 6 (Experimental Procedures), assuming a constant ΔC_p° of $-1.1 \text{ kcal mol}^{-1} \text{ K}^{-1}$ over the temperature range studied.

Table 2: Thermodynamic Properties of the UvrB(Y95W) Interaction with DNA Adduct

parameter	value
ΔC_p° (kcal·mol ⁻¹ ·K ⁻¹)	-1.1 ± 0.01
T_H (°C)	37.2 ± 0.02
T_S (°C)	46.5 ± 0.02
$\Delta G^{\circ}_{\text{obs}}(T_H)$ (kcal·mol ⁻¹)	-10.1 ± 0.04
$\Delta G^{\circ}_{\text{obs}}(T_S)$ (kcal·mol ⁻¹)	-10.2 ± 0.04

2A, the data of $\ln K_{\text{obs}}$ versus $1/T$ were best fitted with eq 1 (see Experimental Procedures), leading to the determination of the heat capacity change ΔC_p° for the binding (Table 2). From this determination, other thermodynamic functions then were calculated, and their relationships with the temperature were plotted in Figure 2B (from eqs 2, 5, and 6).

Several important observations are revealed from the results in Table 2 and Figure 2. First, a large negative value of heat capacity change ΔC_p° ($-1.1 \text{ kcal mol}^{-1} \text{ K}^{-1}$) for the interaction of UvrB(Y95W) with the DNA substrate suggests a significant hydrophobic effect in the specific interaction (10, 11, 19, 20). Second, both standard enthalpy and entropy changes ($\Delta H^{\circ}_{\text{obs}}$ and $T\Delta S^{\circ}_{\text{obs}}$, respectively) vary dramatically as the function of temperature, while the Gibbs free energy ($\Delta G^{\circ}_{\text{obs}}$) is relatively unchanged in contrast. These dramatic variations are the result of a large negative

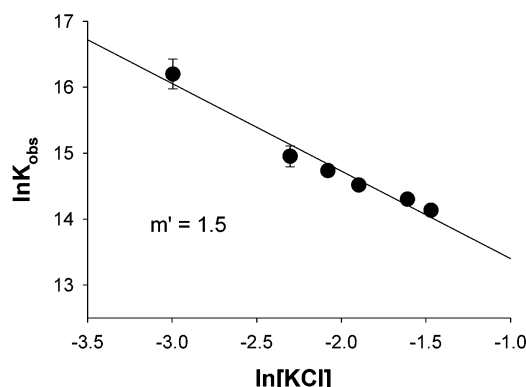


FIGURE 3: Effect of ionic strength on the specific binding of UvrB(Y95W) to the F–30 bp bubble substrate. The damaged DNA (0.1 μM) was mixed with UvrB(Y95W) at 25 °C in binding buffer containing 50 mM Tris-HCl, pH 8.0, 5 mM EDTA, 10 mM MgCl₂, 10% glycerol, and KCl concentrations of 50, 100, 125, 150, 200, or 230 mM. The data were summarized in Table 3 and analyzed as described in Experimental Procedures. The number of ion pairs formed in the complex is estimated to be 1.5, as indicated by m' . The error bars are the standard deviation of at least three independent determinations. The line is a linear least-squares regression analysis of the data.

Table 3: Dependence of the Interaction of UvrB(Y95W) with DNA Adduct on KCl Concentrations at 25 °C

[KCl] (mM)	K_{obs} (M ⁻¹)
50	$10.85 (\pm 2.43) \times 10^6$
100	$3.11 (\pm 0.50) \times 10^6$
125	$2.51 (\pm 0.14) \times 10^6$
150	$2.02 (\pm 0.15) \times 10^6$
200	$1.63 (\pm 0.05) \times 10^6$
230	$1.37 (\pm 0.07) \times 10^6$

value of ΔC_p° as demonstrated by eqs 5 and 6 (see Experimental Procedures). Finally, the values of both $\Delta H^{\circ}_{\text{obs}}$ and $T\Delta S^{\circ}_{\text{obs}}$ remain positive at all physiological temperatures and could only become negative at temperatures higher than 37 °C ($T_H = 37.2$ °C at which $\Delta H^{\circ}_{\text{obs}}$ is zero) and 46 °C ($T_S = 46.5$ °C at which $\Delta S^{\circ}_{\text{obs}}$ equals zero), respectively. Since $\Delta G^{\circ}_{\text{obs}} = \Delta H^{\circ}_{\text{obs}} - T\Delta S^{\circ}_{\text{obs}}$ and a favored $\Delta G^{\circ}_{\text{obs}}$ (<0) for binding can be contributed only from a negative $\Delta H^{\circ}_{\text{obs}}$ and a positive $\Delta S^{\circ}_{\text{obs}}$, the binding of UvrB(Y95W) to the DNA substrate is thermodynamically driven by the entropic effect $\Delta S^{\circ}_{\text{obs}}$ at physiological temperatures; enthalpy made no favorable contributions to the binding.

Ion Effects on the Binding. The effect of ionic strength on molecular and macromolecular interactions has been used widely to estimate the energetic nature of the interactions (12, 27–30). For protein–DNA interactions, the effect reflects the displacement of counterions from the phosphate backbone upon formation of the protein–DNA complex which increases entropy if electrostatic forces are involved in the complex stabilization (12, 14). As the result of this ionic strength effect, the apparent binding constant is dependent on the concentration of salt in the binding buffer, and this relationship can be utilized to determine the effect (see Experimental Procedures) (12, 14). As shown in Figure 3 and Table 3, the $\ln K_{\text{obs}}$ for the binding of UvrB(Y95W) to the F–30 bp bubble substrate has a linear relationship with the natural log of salt concentrations [KCl] from 50 to 230 mM. Linear regression of the data generates a slope from which the average number of ions released ($m' = 1.5$) in this specific binding was determined. In contrast to the

contact size of 24 bp for the binding of UvrB to the BPDE–DNA substrate (mediated by UvrA) determined by DNase I footprinting (21), this number of ions released is relatively small. This supports that other nonelectrostatic forces may be largely involved in the complex formation in addition to the ionic interactions.

The nonelectrostatic contributions to the free energy of binding could be estimated using the equation:

$$\Delta G_{\text{ne}}^{\circ} = \Delta G_{\text{obs}}^{\circ}(1 \text{ M } \text{M}^{+}) - N\Delta G_{\text{Lys}}^{\circ}$$

where the M^{+} stands for the monovalent metal ion of the salt (12, 22), $\Delta G_{\text{obs}}^{\circ}(1 \text{ M } \text{M}^{+})$ is the standard free energy at $[\text{M}^{+}] = 1 \text{ M}$, determined by extrapolation from the plot of $\ln K_{\text{obs}}$ versus $\ln [\text{M}^{+}]$ to 1 M, N is the number of ion pairs, and $\Delta G_{\text{Lys}}^{\circ}$ is the standard free energy of formation of a single lysine–phosphate ionic interaction. In the present study, the value of $\Delta G_{\text{obs}}^{\circ}(1 \text{ M } \text{K}^{+})$ is about $-7.0 \text{ kcal}\cdot\text{mol}^{-1}$, and the $\Delta G_{\text{Lys}}^{\circ}$ is $0.2 \text{ kcal}\cdot\text{mol}^{-1}$ at $[\text{K}^{+}] = 1 \text{ M}$ (12, 23), assuming that Na^{+} and K^{+} have equivalent effects on the binding. As an estimate, it is assumed that N is equivalent to the ions released. Therefore, $\Delta G_{\text{ne}}^{\circ} = -7.3 \text{ kcal}\cdot\text{mol}^{-1}$, indicating that under our standard binding conditions about 76% of the total free energy ($-9.6 \text{ kcal}\cdot\text{mol}^{-1}$) for the specific binding of UvrB(Y95W) to the F–30 bp DNA substrate is contributed by nonelectrostatic interactions.

DISCUSSION

Determination of the biochemical properties of DNA damage recognition by UvrB is an important step toward the understanding of mechanistic details of nucleotide excision repair in *E. coli*. In the present study, we have defined the thermodynamic characteristics of the UvrB–(Y95W) interaction with a structure-specific DNA adduct in the absence of UvrA using rigorous fluorescence spectroscopic methods. The UvrB(Y95W) mutant protein bypassed the requirement of UvrA for its binding to DNA substrates, which opened an avenue for the direct examination of UvrB–DNA adduct interactions. Our study provides an important insight into the biochemical basis that governs DNA damage recognition in NER in general.

To examine DNA damage recognition by UvrB, fluorescence quenching studies of site-specific UvrB mutants were performed in the presence and absence of DNA substrate. The use of the polar but uncharged acrylamide quencher ensured the measurement of the molecular accessibility of specific residues by avoiding possible electronic interference of charged surroundings. Acrylamide can quench both exposed and partially buried tryptophans. Consistent with the UvrB structures of *B. caldotenax* and *T. thermophilus* (5–7) and the results reported earlier for *E. coli* UvrB (26), data from the site-specific quenching experiments indicate that the amino acid at residue 95 is more exposed than at residues 92 and 101. More importantly, upon binding to DNA, the acrylamide accessibility to residue 95 was significantly reduced, an indication of direct involvement of this residue in the DNA interactions. These results confirm the unique role of residue 95 in UvrB recognition of DNA damage.

Data from our temperature dependence study indicated that the interaction of UvrB(Y95W) with the DNA adduct

produced a large negative heat capacity change, $\Delta C_p^{\circ} = -1.1 \text{ kcal}\cdot\text{mol}^{-1}\cdot\text{K}^{-1}$ (Table 2). Binding of many proteins to specific DNA sequences has been characterized by large negative heat capacity changes (19). It is believed that this large negative ΔC_p° resulted from the hydrophobic interactions which bury the nonpolar surface of the forming complex and reduce exposure to water (10, 18, 19). The process may couple with a combination of local folding of protein, DNA helix unwinding, and changes in base stacking (19, 24). Thermodynamics of this process also are featured with the highly temperature-dependent enthalpic and entropic components of the free energy (Figure 3). The values of both components linearly decreased with the temperature. In the range of physiological temperatures, interaction of UvrB–(Y95W) with the DNA substrate is stabilized by entropic effects as both the $\Delta H_{\text{obs}}^{\circ}$ and $T\Delta S_{\text{obs}}^{\circ}$ remain positive in this range. On the other hand, the electrostatic forces involved in the UvrB(Y95W)–DNA interaction were assessed by examining the ion effect on equilibrium binding constants in this study. The relatively small number of ions released upon the binding of the UvrB mutant to the fluorescein-damaged DNA (Figure 3) supports the notion that the binding is likely driven predominantly by nonelectrostatic forces. An extrapolation to a 1 M salt concentration indicates that about 76% of the total favorable free energy change for stabilizing the complex formation comes from nonelectrostatic contributions, albeit the determination was based on a couple of assumptions (12–13, 18, 23). All of these results confirm that a major driving force for the specific binding of UvrB(Y95W) to the DNA adduct is hydrophobic interaction.

As a NER protein, UvrB recognizes DNA adducts through the mediation of UvrA, a molecular matchmaker. The lack of direct interaction of native UvrB with DNA or the DNA adduct and the requirement of DNA strand opening for the damage recognition by UvrB (to expose the buried adduct and/or bases) support a minimal role of electrostatic energy in UvrB interaction with the DNA adduct. UvrB is known to cause unwinding and bending of the DNA helix upon binding to damage driven by UvrA (25). In this case, hydrophobic interactions with the bases and adduct could provide increased affinity and, therefore, could contribute to the large negative heat capacity change observed in the present experiments. The dramatic enhancement of UvrB affinity for DNA substrate due to a single and more hydrophobic mutation is obviously a piece of evidence to support a dominant role of hydrophobicity in the DNA damage recognition of UvrB. However, it should be noted that since a mutant protein was used in this study, the extent of hydrophobic forces involved in the native UvrB interaction with the DNA adduct could be relatively smaller due to the hydrophobic difference between a tyrosine and a tryptophan. Despite this, the thermodynamic characteristics determined in the present study likely reflect the parameters of the native protein–DNA interaction, including significant global and local structural and biochemical changes of both protein and DNA with the involvement of many other residues and nucleotides. It also is important to note that the UvrB(Y95W) protein functions as well as the native UvrB in the UvrABC incisions (26). Therefore, the conclusion of this study is significant to the normal process of NER.

ACKNOWLEDGMENT

We thank Dr. Phillip Musich for critical reading of the manuscript.

REFERENCES

1. Van Houten, B. (1990) *Microbiol. Rev.* 54, 18–51.
2. Sancar, A. (1996) *Annu. Rev. Biochem.* 65, 43–81.
3. Lindahl, T., and Wood, R. D. (1999) *Science* 286, 1897–1905.
4. Zou, Y., Luo, C., and Geacintov, N. E. (2001) *Biochemistry* 40, 2923–2931.
5. Theis, K., Chen, P. J., Skovvaga, M., Van Houten, B., and Kisker, C. (1999) *EMBO J.* 18, 6899–6907.
6. Machius, M., Henry, L., Palnitkar, M., and Deisenhofer, J. (1999) *Proc. Natl. Acad. Sci. U.S.A.* 96, 11717–11722.
7. Nakagawa, N., Sugahara, M., Masui, R., Kato, R., Fukuyama, K., and Kuramitsu, S. (1999) *J. Biochem.* 126, 986–990.
8. Baldwin, R. L. (1986) *Proc. Natl. Acad. Sci. U.S.A.* 83, 8069–8072.
9. Bechtel, W. J., and Schellman, J. A. (1987) *Biopolymers* 26, 1859–1877.
10. Ha, J.-H., Spolar, R. S., and Record, M. T., Jr. (1989) *J. Mol. Biol.* 209, 801–816.
11. Record, M. T., Jr., Ha, J.-H., and Fisher, M. A. (1991) *Methods Enzymol.* 208, 291–343.
12. Record, M. T., Jr., Lohman, T. M., and deHaseth, P. (1976a) *J. Mol. Biol.* 107, 145–158.
13. Record, M. T., Jr., Woodbury, C. P., and Lohman, T. M. (1976b) *Biopolymers* 15, 893–915.
14. Record, M. T., Jr., deHaseth, P. L., and Lohman, T. M. (1977) *Biochemistry* 16, 4791–4796.
15. Lakowicz, J. R. (1999) *Principles of Fluorescence Spectroscopy*, 2nd ed., Kluwer Academic/Plenum Publishers, New York.
16. Eftink, M. R., and Ghiron, C. (1981) *Anal. Biochem.* 114, 199–227.
17. Eftink, M. R. (1991) *Biophysical and Biochemical Aspects of Fluorescence Spectroscopy* (Dewey, T. G., Ed.) pp 1–41, Plenum Press, New York.
18. Zou, Y., Bassett, H., Walker, R., Bishop, A., Amin, S., Geacintov, N. E., and Van Houten, B. (1998) *J. Mol. Biol.* 281, 107–119.
19. Spolar, R. S., and Record, M. T. (1994) *Science* 11, 777–784.
20. Von Hippel, P. H. (1994) *Science* 11, 769–770.
21. Zou, Y., Liu, T.-M., Geacintov, N. E., and Van Houten, B. (1995) *Biochemistry* 34, 13582–13593.
22. Terry, B. J., Jack, W. E., Rubin, R. A., and Modrich, P. (1983) *J. Biol. Chem.* 258, 9820–9825.
23. Lohman, T. M., deHaseth, P. L., and Record, M. T., Jr. (1980) *Biochemistry* 19, 3522–3530.
24. Petri, V., Hsieh, M., and Brenowitz, M. (1995) *Biochemistry* 34, 9977–9984.
25. Verhoeven, E. E., Wyman, C., Moolenaar, G. F., and Goosen, N. (2002) *EMBO J.* 21, 4196–4205.
26. Zou, Y., Ma, H., Minko, I. G., Shell, S. M., Yang, Z., Qu, Y., Xu, Y., Geacintov, N. E., and Lloyd, R. S. (2004) *Biochemistry* 43, 4196–4205.
27. Lohman, T. M., deHaseth, P. L., and Record, M. T., Jr. (1980) *Biochemistry* 19, 3522–3530.
28. Winter, R. B., and von Hippel, P. H. (1981) *Biochemistry* 20, 6948–6960.
29. Terry, B. J., Jack, W. E., Rubin, R. A., and Modrich, P. (1983) *J. Biol. Chem.* 258, 9820–9825.
30. Record, M. T., Jr., Ha, J. H., and Fisher, M. A. (1991) *Methods Enzymol.* 208, 291–343.

BI0359933